Perceptibility of Non-sinusoidal Bands

Wencheng Wu, Edul N. Dalal, and D. René Rasmussen
Xerox Corporation
Webster, New York

Abstract

A common type of image quality problem involves the presence of periodic light and dark bands on an image that is meant to be uniform. Much work has been done on measuring the perceptibility of sinusoidal and square-wave bands and it is known that the sensitivity to these two types of bands with the same periodicity could vary quite significantly. This is especially true when the periodicity of the banding is large. However, it is not clear how to evaluate banding of large periodicity that is neither sinusoidal nor square-wave.

In this work, we report on a study investigating the perceptibility and objectionability of non-sinusoidal bands via psychophysical experiments. More specifically, we estimate the relative objectionability of sinusoidal bands and various types of non-sinusoidal bands. This will focus on bands with large periodicity, since the perceptibility of these bands varies the most depending on the "shape" of the band's profile. Our objectives are to assess the differ-ence in objectionability among various types of nonsinu-soidal bands and to apply the psychophysical data as a correction factor on the objectionability curve of sinusoidal bands.

1. Introduction

A common type of image quality problem involves the presence of periodic light and dark bands on an image that is meant to be uniform. This artifact is often referred to banding. Much research has been done to model[1] and reduce this artifact[2]. To evaluate the progress of the system development, it is very important to have an assessment of the perceptibility of the banding defect when it is near threshold level, or the objectionability when it is visible[3, 4]. The most common approach to these tasks is via visual inspection, which is labor intensive and subjective. Another common approach is to use the amplitude in the frequency domain as a measure of the objectionability. This involves measuring the perceptibility and objection-ability at various frequencies, coupled with a Fourier analysis.

Much work has been done on measuring the perceptibility of sinusoidal and square-wave bands and it is known that the sensitivity to these two types of bands with the same periodicity can vary quite significantly[5]. This is especially true when the periodicity of the banding is large. However, it is not clear how to evaluate banding of large periodicity that is neither sinusoidal nor square-wave.

In this work, we report on a study investigating the perceptibility and objectionability of non-sinusoidal bands via psychophysical experiments. More specifically, we estimate the relative objectionability of sinusoidal bands and various types of non-sinusoidal bands. This will focus on bands with large periodicity, since the perceptibility of large periodicity bands has the greatest dependency on the "shape" of the band's profile. Our objectives are to assess the difference in objectionability among various types of non-sinusoidal bands and to apply the psychophysical data as a correction factor to the objectionability of sinusoidal bands of the same periodicity.

This paper is organized as follows. In Sec. 2, we will briefly describe the psychophysical experiments that we conducted for this study. In Sec. 3, methods for estimating the objectionability of non-sinusoidal bands will be presented. Finally, conclusions will be drawn in Sec. 4.

2. Psychophysical Experiment

In this section, we describe the psychophysical experiment for measuring the objectionability of the bands. Our objective is to investigate the impact of the shape of the profile on the visual rating of the objectionability of prints containing these bands.

2.1 Test Samples

In order to create different banding profiles, we first generated various shapes of profile mathematically (see Appendix for details). Figure 2 shows some example banding profiles that were used in this experiment. These banding profiles with random phase were then applied, using an image simulation tool developed internally at Xerox, to create images with banding. For each simulated image the image area is a $180mm \times 240mm$ uniform gray containing bands at various levels of ΔL^* mean-to-peak amplitude. The bands were aligned parallel to the short edge of the image. The intended average L^* of all simulated images was set to 50. These simulated images were printed on a calibrated imagesetter[*] to form the test sample set. Each test sample was assigned a 3-digit randomized print identification number (PID) and mounted on an acid-free foam-board. An illustration of a mounted sample is shown in Fig. 2. The characteristics of all banding profiles in the test sample set are listed in Table 1.

[*] Avantra 20, Agfa

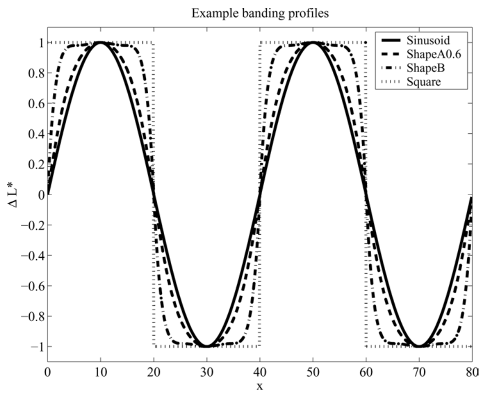

Figure 1. Example profiles for creating banding prints

Table 1. The Characteristics of the Banding Prints Used in this Study

Shape (f_0)	mean-to-peak amplitude in L* unit
Sinusoid(0.025)	0.1, 0.2, 0.4, 0.5, 0.8, 1
ShapeA$_{0.6}$(0.025)	0.235, 0.471, 0.589, 0.823
Square(0.025)	0.1, 0.15, 0.2, 0.25, 0.3
Sinusoid(0.05)	0.1, 0.3, 0.5, 0.6, 0.8
ShapeA$_{0.6}$(0.05)	0.118, 0.235, 0.353, 0.471, 0.588
ShapeB(0.05)	0.1, 0.15, 0.25
Square(0.05)	0.1, 0.15, 0.2, 0.25, 0.3
Sinusoid(0.5)	0.3, 0.4
Square(0.5)	0.3

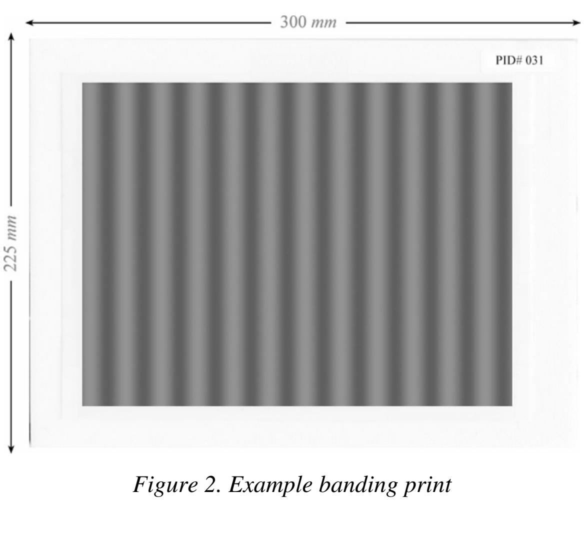

Figure 2. Example banding print

2.2 Procedure

We applied the graphical rating scale method[6] (with anchors) for this survey. The anchor prints were pre-selected by the designers of the experiment, where the rating-0 anchor was a print without bands and the rating-8 anchor was a print with severe banding, Sinusoid (0.05*c/mm*) with mean-to-peak ΔL^* amplitude = 0.8. The experimental procedure was as follows. Prior to each session, the order of the samples was randomized. The subject was then asked to rate print samples one at a time against the anchor prints until all prints are evaluated. Note that during the experiment the subject was not allowed to go back and review or re-rate prints that he/she has already evaluated. Note also that the visual rating (VR) is an impairment measure of banding artifacts; the larger the VR, the more objectionable the banding.

2.3 Result and Discussion

Seventeen subjects have participated in this experiment. The experimental results are shown in Fig. 3. We will refer to each curve in this figure as the *visual rating curve* of the band with a given profile shape and fundamental frequency. From the results, it can be seen that for a given shape of bands with fixed periodicity the VR increases almost linearly with the amplitude of the band except at large amplitudes.

From Figs. 3a and 3b, it is observed that the supra-threshold sensitivity (slope) of the non-sinusoidal bands is quite different from that of the sinusoidal bands; and the lower the fundamental frequency, the larger the difference. Note also that the supra-threshold sensitivity depends on the shape of the bands. In the next section, we will describe how these psychophysical data were used to compensate for this sensitivity difference due to the shape of the band.

3. Methods for Estimating Objectionability of Non-Sinusoidal Bands

In this section, we propose an approach to estimate the objectionability of non-sinusoidal bands. This approach treats high-frequency and low-frequency bands differently. The term *low-frequency* is used to describe the frequency range where the contribution of harmonics[5] is not negligible.

To illustrate that, we re-plot in Fig. 4 the contrast sensitivity data from Ref. 5, converting the frequency unit from *cpd* (cycle per degree) to *c/mm* at normal viewing distance (400 mm). As discussed by Campbell et al[5] the sensitivity of square bands is about $4/\pi$ times that of sinusoidal bands, for high spatial frequency gratings (frequencies at 0.08*c/mm* or higher). We will denote this frequency 0.08*c/mm* as the cut-off frequency f_C. When the fundamental frequency f_0 of a band is higher than f_C, it is reasonable to use solely the magnitude of the fundamental frequency as a measure of objectionability of the banding (as mentioned in Ref. 5). Our experimental result shown in Fig. 3c agrees with this assumption. That is, the VR=5.3 of Square(0.5*c/mm*) with 0.3ΔL^* amplitude is very close to the interpolated VR=5.4 of Sin(0.5*c/mm*) with ($0.3 \bullet 4/\pi$) ΔL^* amplitude.

When the fundamental frequency is lower than f_C, this is no longer true as illustrated in Fig. 4 where the sensitivity ratio increases as f_0 decreases. This is the main reason why we focus on low frequencies where the contribution of harmonics is significant.

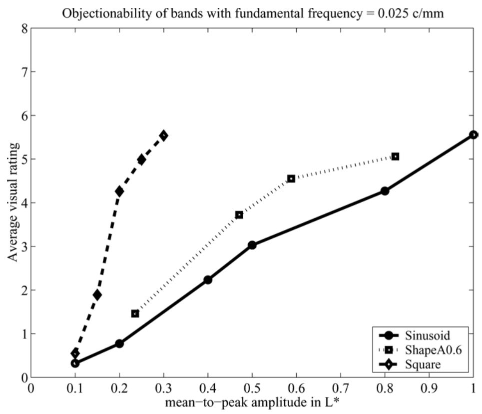

(a)

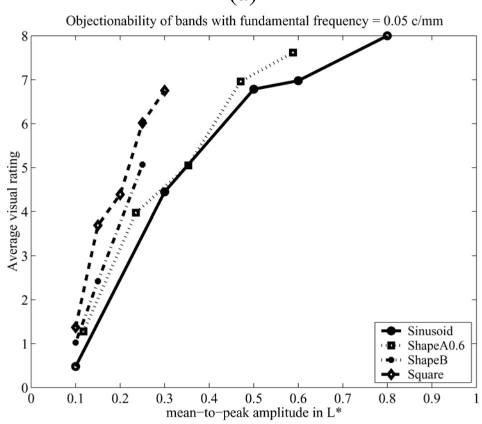

(b)

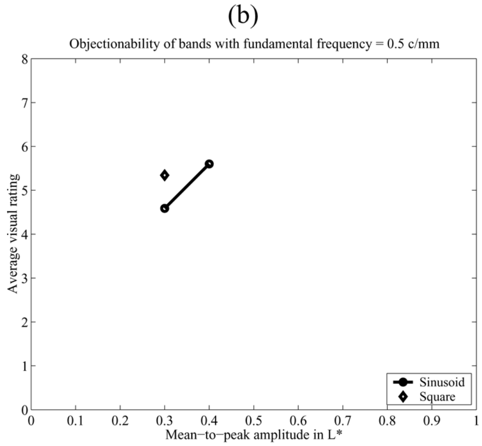

(c)

Figure 3. Experimental results: (a) objectionability data on 0.025c/mm bands, (b) objectionability data on 0.05c/mm bands, and (c) objectionability data on 0.5c/mm bands

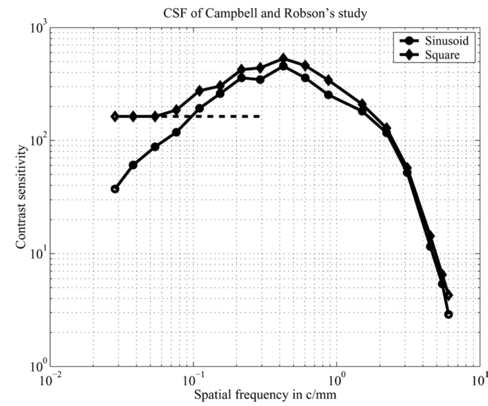

Figure 4. Illustration of the contrast sensitivity function using data from Campbell and Robson's study.[5]

3.1 Relative Sensitivity of Non-Sinusoidal Bands

Since the experimental results (see Fig. 3a and 3b) show that for a given fundamental frequency the shape of all visual rating curves is nearly the same, all approximately linear prior to saturation, it is reasonable to assume that the relative sensitivity is independent of the mean-to-peak amplitude. Hence we can define a relative sensitivity that is independent of mean-to-peak amplitude. That is, let us define R to be the relative objectionability of a banding profile with fundamental frequency f_0.

$$R(f_0) = \frac{\text{VR of the given banding profile}}{\text{VR of the corresponding sinusoidal profile}} \qquad (1)$$

Here, the corresponding sinusoidal profile has the same f_0 and mean-to-peak amplitude as that of the given banding profile.

From the data in Fig. 3, it is observed that all visual rating curves intersect approximately at the same point on L^* axis for a given fundamental frequency. This intersection L^* value can be interpreted as the threshold, or minimum value that is perceptible. It would appear from Fig. 3a and 3b that, at a given fundamental frequency, the threshold is independent of the banding profile, whereas the suprathreshold sensitivity clearly depends on the profile. Further experiments are required to probe this effect in more detail, and we plan to conduct them. This would be a significant observation if it can be validated.

To measure the $R(f_0)$, we first utilize this observation and perform least-square linear fits to all visual rating curves with a constant intersection on the L^* axis. We then compute the ratio of slopes between a given band and a sinusoid with the same f_0, and use that as $R(f_0)$. Table 2 summarizes the results. In the next sub-section, we will utilize these results to compensate for the difference between non-sinusoidal bands and sinusoidal bands.

Table 2. Measurement of Relative Sensitivity to the Corresponding Sinusoid.

Shape (f_0)	model of visual rating curve	$R(f_0)$
Sinusoid(0.025)	$6.0076(x-0.0593)$	1
ShapeA$_{06}$(0.025)	$7.5778(x-0.0593)$	1.2614
Square(0.025)	$24.8177(x-0.0593)$	4.1311
Sinusoid(0.05)	$13.4024(x-0.0277)$	1
ShapeA$_{06}$(0.05)	$14.8886(x-0.0277)$	1.1109
ShapeB(0.05)	$21.5039(x-0.0277)$	1.6045
Square(0.05)	$25.8517(x-0.0277)$	1.9289

3.2 Profile-Analysis Approach

First, let us define similarity S of a banding profile with fundamental frequency f_0,

$$S = \frac{2\pi f_0 \cdot (\text{mean} - \text{to} - \text{peak amplitude})}{\text{max. slope of the banding profile}} \qquad (2)$$

as a measure of how similar this band profile is to a sinusoid. It can be shown that $S(f_0) = 1$ for sinusoidal profile, and $S(f_0) = 0$ for square-wave profile. It can be shown that S lies between 0 and 1, and is independent of f_0 and mean-to-peak amplitude for any given non-sinusoidal profile generated from the Appendix.

From the results in Sec. 2.3. it is obvious that $R(f_0)$ defined in Eq. (1) varies with f_0. In order to model this f_0-dependency, we utilize the following two observations from Campbell and Robson's study[5]:

1. The sensitivity of *low-frequency* square bands, $f_0 \le f_C$, is near constant.
2. The sensitivity of *low-frequency* sinusoidal bands, $f_0 \le f_C$, is near linear to $\log f_0$

from which we can infer that this dependency is exponential. Note that these two trend lines (see dotted line in Fig. 4) meet at roughly 0.1*c/mm*. Thus we further define a frequency-scaled relative objectionability ρ as

$$\rho = (R(f_0))^{(f_0/0.1)}. \qquad (3)$$

This ratio should now be (nearly) independent of f_0.

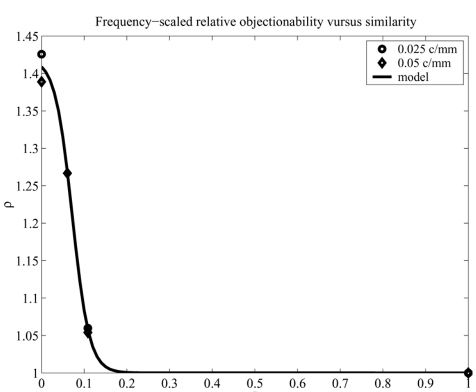

Figure 5. Frequency-scaled relative sensitivity versus similarity at 0.025 and 0.05c/mm

Figure 5 shows the relationship between similarity S and frequency-scaled relative objectionability ρ using $R(f_0)$ in Table 2. It can be modeled by a sigmoid function:

$$\rho = 1 + \frac{0.42}{1 + e^{50(S-0.072)}} \qquad (4)$$

At this point, we have established a method to estimate the objectionability of a print with non-sinusoidal banding via the objectionability of the corresponding sinusoidal print. This approach is summarized in Table 3.

Table 3. Summary of the Profile-Analysis Approach

Profile-analysis approach:
1. Compute similarity S using Eq.(2).
2. Compute frequency-scaled relative objectionability ρ using Eq.(4).
3. Compute relative objectionability R using Eq.(3).
4. Compute VR of the print using Eq.(1).

4. Conclusion

In this paper, we investigate the objectionability of nonsinusoidal bands via psychophysical experiment. From the results, it is evident that there is a substantial difference between non-sinusoidal bands and sinusoidal bands especially in the low frequency range. To take into account this difference, we have proposed a profile-analysis approach using a sigmoid model between frequency-scaled relative sensitivity and the similarity to sinusoids. This model can be applied to estimate the objectionability of non-sinusoidal bands from that of sinusoidal bands, for which many studies are available in the literature. This model fits well on the limited data that we have and appears to be promising. Further research with larger sample sets is required to validate the model.

Acknowledgements

We would like to thank all subjects that participated in this experiment and special thanks to Cindy Blair for managing the survey.

References

1. R. Loce, W. Lama, and M. Maltz, "Modeling vibration induced halftone banding in a xerographic laser printer," *Journal of Electronic Imaging*, vol. 4, no. 1, pp. 58 – 61, 1995.
2. G.-Y. Lin, J. M. Grice, J. P. Allebach, G. Chiu, W. Bradburn, and J. Weaver, "Banding artifact reduction in electrophotographic printers by using pulse width modulation," *Proceedings of IS&T's NIP16: International Conference on Digital Printing Technologies*, Vancouver, B.C., Canada, November, 2000, pp 281– 286.

3. D. R. Rasmussen, E. N. Dalal, and K. M. Hoffman, "Measurement of macro-uniformity: Streaks, bands, mottle and chromatic variations," *Proceedings of the 2001 IS&T International Image Processing, Image Quality, Image Capture Systems Conference*, Montr´eal, Quebec, Canada, April 2001, pp 90 – 95.
4. J. C. Briggs, M. Murphy, and Y. Pan, "Banding characterization for inkjet printing," *Proceedings of the 2000 IS&T International Image Processing, Image Quality, Image Capture Systems Conference*, Portland, OR, March 2000, pp 84 – 88.
5. F. W. Campbell and J. G. Robson, "Application of Fourier analysis to the visibility of gratings," *Journal of Physiology (London)*, vol. 197, pp. 551 – 566, 1968.
6. P. G. Engeldrum, *Psychometric Scaling: A Toolkit for Imaging Systems Development*. Imcotek Press, 2000.

Appendix

In this work, we focus on those non-sinusoidal profiles that have the same symmetric properties possessed by sinusoids and square-waves, i.e. symmetric at half period, at 1⁄4 period, and at 3⁄4 period (see Fig. 2). The banding profiles which were used in sample creation for the psychophysical experiments are:

Sinusoid(f_0): $y(x; f_0) = \sin(2\pi f_0 x)$. (A-1)

Square(f_0):

$$y(x;f_0) = \begin{cases} 1 & \mathrm{mod}(f_0 x) \le 0.5 \\ -1 & \text{otherwise.} \end{cases} \quad \text{(A-2)}$$

ShapeA$_\alpha$(f_0): (A-3)

$$y(x;\alpha,f_0) = \frac{4}{\pi}\sum_{n=0}^{25} \frac{e^{-\frac{2n(1-\alpha)}{\alpha}}}{2n+1}\sin((4n+2)\pi x f_0).$$

ShapeB(f_0): (A-4)

$$y(x; f_0) = (-1)^n(1 - 0.106388\theta^2 + 0.199779\theta^4 - 0.130077\theta^6),$$
with $n = \mathrm{floor}(2xf_0 + 0.5)$, $\theta = 2\pi x f_0 - n\pi$.

where, x is the distance from the origin of the band profile in *mm*; and f_0 is the fundamental frequency of the band in *c/mm*. The function floor(x) returns the integer that is closest to x but no greater than x. The function mod(x) equals x - floor(x). In the case of ShapeA, α is the parameter that governs the shape of the collection of ShapeA banding. Note that for simplicity, we did not introduce a phase term into the above equations. But in practice, the phase of the profile can be varied by shifting its origin from x to ($x - x_0$).

Biography

WenchengWu received his Ph.D. in Electrical Engineering from Purdue University, Indiana, in 2000. He is currently a member of Xerox Corp.'s Wilson Center for Research and Technology working on the development of print quality metrics.

Edul N. Dalal joined Xerox Corp. in 1983 with a PhD in Materials Science. He is currently a Research Fellow as well as Technical Manager of the System Image Quality area at the Wilson Center for Research and Technology in Webster, NY. His research interests include Image Quality, Color Science, Polymer Physics and Surface Science.

D. Ren´e Rasmussen received his PhD in physics from the Niels Bohr Institute, Copenhagen, in 1990. He is Principal Scientist at Xerox Corp. and leads a project on development of Xerox internal standards for color image quality assessment. He has been with Xerox Corp. since 1992.